THE CLUSTERING ANNULAR FLOW MODEL OF CIRCULATING FLUIDIZED BEDS

HIROYUKI ISHII, TAKASHI NAKAJIMA AND MASAYUKI HORIO

Department of Applied Chemistry for Resources, Tokyo University of Agriculture and Technology, Tokyo 184

Key Words: Fluidization, Flow Modeling, Circulating Fluidized Beds, Cluster, Solid Flow, Cluster Size

The Clustering Annular Flow Model (CA model) is presented to describe the annular flow structure in the main column of a circulating fluidized bed (CFB). With the present model the flow parameters for a CFB including the dimensionless radius of the core α can be estimated, given the values of both the diameter and the voidage of the cluster phase.

The model was successfully validated by comparison of values of α experimentally determined with those predicted from the model and observed cluster parameters. With consideration of the cluster formation it became possible to give a quantitative explanation of the annular flow structure and the high gas-solid slip velocity so far observed in circulating fluidized beds.

Introduction

Circulating fluidization has a number of advantages such as good gas-solid contact, capability of handling fine particles under severe elutriation, a wide operating range and large gas throughput. Regarding the hydrodynamic features of a circulating fluidized bed, to date the large gas-solid slip velocity,[17] cluster formation,[6,8,16] sigmoidal axial distribution of solid holdup,[8] and solid downflow over the wall[2,4,6,15] have been reported. Among them the last item seems to be the most significant. Solid downflow is a dominant factor in combustor design and scale-up since it controls the bed-to-wall heat transfer coefficients. Nevertheless, information sufficient to predict solid downflow characteristics has not been established.

For the riser of a pneumatic conveying line, Nakamura and Capes presented a model (NC model) to predict the annular flow behavior of particles assuming that particles are suspended homogeneously. They used the Richardson-Zaki correlation for the velocity-voidage relationship where the local gas-solid slip velocity is always less than the particle terminal velocity u_t. However, as investigated by Grace and Tuot[3] using the Anderson-Jackson model,[1] a homogeneous particle suspension is always unstable. They have also shown that the growth distance of disturbances decreases with increasing suspension density, i.e. the suspension becomes more unstable as its density increases. Therefore, the clustering nature seems to be essential for a suspension in circulating fluidized beds and the local slip velocity is likely to exceed the particle terminal velocity.

Concerning the flow modeling of such a clustering suspension a direct numerical simulation such as that by Pritchett *et al.*[12] for bubbling fluidization is possible only theoretically. The lack of knowledge of how to treat the turbulence energy dissipation of rather dense suspensions would present a great difficulty in such an approach. Therefore, for the time being an approximate approach is the only way to obtain practically applicable results from modeling.

Yerushalmi *et al.*[16] tried to estimate the average drag coefficient of a clustering suspension assuming that clusters were uniform in shape (spherical), size, voidage and velocity and that the voidage in the cluster phase was ε_{mf}. However, no attempt has been made to extend such an approximate approach to account for the annular flow field in a circulating fluidized bed.

In the present work the clustering annular flow typical in circulating fluidized beds is analyzed on the basis of (1) an approximate expression for the drag acting on clusters and (2) the minimum pressure gradient principle which was previously used by Nakamura and Capes.[10]

1. Clustering Annular Flow Model (CA model)

1.1 Assumptions

The following assumptions were made for the formulations:

1) The solid suspension in a circulating fluidized bed consists of denser islands and a leaner continuous network. The denser islands are called clusters.
2) The drag coefficient of the cluster can be estimated from the spherical cluster approximation.

Received September 29, 1988. Correspondence concerning this article should be addressed to M. Horio. H. Ishii is now with Idemitsu Engineering Co., Ltd., Chiba 260.

3) Particles in the dilute phase can be neglected in the material balance.
4) In a cluster the gas moves with the cluster and particles are uniformly suspended.
5) Solids are ascending in the core and descending in the annulus.
6) Clusters are homogeneously suspended both in the core and in the annulus.
7) The following modified Richardson-Zaki (R-Z) equation[13] is applicable to a cluster:

$$u'-v'=u_{tcl}\varepsilon^{*n}/\varepsilon \tag{1}$$

The most significant difference of the present model from Yerushalmi *et al.*[16] model is that in the present model annular flow is an essential assumption. Furthermore, in the present model the voidages in the cluster $\varepsilon_{cl,c}$ and $\varepsilon_{cl,a}$ are treated as variables for clusters in the core and in the annulus respectively.

1.2 Material balance

From the material balance we have:
total gas flow:

$$u_0=\alpha^2 u_c+(1-\alpha^2)u_a \tag{2}$$

gas flow in core and annulus:

$$u_X=u'_X\varepsilon^*_X+v'_X(1-\varepsilon^*_X)\varepsilon_{cl,X} \tag{3}$$

total solid flow:

$$v_0=\alpha^2 v_c+(1-\alpha^2)v_a \tag{4}$$

solid flow in core and annulus:

$$v_X=v'_X(1-\varepsilon^*_X)(1-\varepsilon_{cl,X}) \tag{5}$$

cross section average void fraction:

$$\bar{\varepsilon}=\alpha^2\varepsilon_c+(1-\alpha^2)\varepsilon_a \tag{6}$$

void fraction in core and annulus:

$$\varepsilon_X=1-(1-\varepsilon^*_X)(1-\varepsilon_{cl,X}) \tag{7}$$

where $X=c,\ a$

1.3 Momentum balance

From the momentum balance for gas and solid we have:
core gas momentum equation:

$$\rho_f\varepsilon^*_c\frac{d(u'^2_c)}{dz}=-\varepsilon^*_c\frac{dP}{dz}-\beta_c(u'_c-v'_c)^2 \tag{8}$$

core solid momentum equation:

$$\rho_{cl}(1-\varepsilon^*_c)\frac{d(v'^2_c)}{dz}=-(1-\varepsilon^*_c)\frac{dP}{dz}+\beta_c(u'_c-v'_c)^2-\frac{4\tau_a}{\alpha D_t}-\rho_{cl}(1-\varepsilon^*_c)g \tag{9}$$

annulus gas momentum equation:

$$\rho_f\varepsilon^*_a\frac{d(u'^2_a)}{dz}=-\varepsilon^*_a\frac{dP}{dz}-\beta_a(u'_a-v'_a)^2-\frac{4\tau_f}{(1-\alpha^2)D_t} \tag{10}$$

annulus solid momentum equation:

$$\rho_{cl}(1-\varepsilon^*_a)\frac{d(v'^2_a)}{dz}=-(1-\varepsilon^*_a)\frac{dP}{dz}+\beta_a(u'_a-v'_a)^2+\frac{(4\alpha\tau_\alpha-4\tau_p)}{(1-\alpha^2)D_t}-\rho_{cl}(1-\varepsilon^*_a)g \tag{11}$$

In the following a quasi-steady state is assumed at any height. Therefore, accumulation terms in Eqs. (8)–(11) (i.e. the left-hand sides of the equations) are neglected.

1.4 Gas-cluster friction factors β_c, β_a and R-Z Equation

From assumption 7) we can write the following equation for the core and annulus regions:

$$u'_X-v'_X=u_{tcl,X}\varepsilon^{*n}_X/\varepsilon_X \quad (X=c,a) \tag{12}$$

By using Eq. (12) the friction factors β_c and β_a in the momentum balance equations can be determined. First by eliminating dP/dz between Eqs. (8) and (9) we have Eq. (13) and in the same manner from Eqs. (10) and (11) we have Eq. (14).

$$u'_c-v'_c=\frac{\rho_{cl}g\varepsilon^*_c(1-\varepsilon^*_c)}{\beta_c}\left\{1+\frac{4\tau_\alpha}{(1-\varepsilon^*_c)\alpha D_t\rho_{cl}g}\right\} \tag{13}$$

$$u'_a-v'_a=\frac{\rho_{cl}g\varepsilon^*_a(1-\varepsilon^*_a)}{\beta_a}\left\{1+\frac{4(\tau_p-\alpha\tau_\alpha)}{(1-\varepsilon^*_a)(1-\alpha^2)D_t\rho_{cl}g}\right\} \tag{14}$$

Nakamura and Capes[10] assumed that the term $4\tau_\alpha/(1-\varepsilon^*_c)\alpha D_t\rho_{cl}g$ was sufficiently smaller than unity. However, as is examined later, this assumption is quite doubtful. Therefore, in the present analysis τ_α is not neglected.

Substituting Eq. (12) into Eqs. (13) and (14) we have the following expressions for β_c and β_a:

$$\beta_c=\frac{\rho_{cl}g\varepsilon^*_c(1-\varepsilon^*_c)}{(u_{tcl,c}\varepsilon^{*n}_c/\varepsilon_c)^2}\left\{1+\frac{4\tau_\alpha}{(1-\varepsilon^*_c)\alpha D_t\rho_{cl}g}\right\} \tag{15}$$

$$\beta_a=\frac{\rho_{cl}g\varepsilon^*_a(1-\varepsilon^*_a)}{(u_{tcl,a}\varepsilon^{*n}_a/\varepsilon_a)^2}\left\{1+\frac{4(\tau_p-\alpha\tau_\alpha)}{(1-\varepsilon^*_a)(1-\alpha^2)D_t\rho_{cl}g}\right\} \tag{16}$$

1.5 Expression for shear stress τ_p

From the previous work on pneumatic conveying the wall-solid shear stress τ_p can be expressed as

$$\tau_p=\frac{1}{2}f_p(1-\varepsilon)\rho_p|v'_a|v'_a \quad (f_p=a|v'_a|^b) \tag{17}$$

In the Konno and Saito[7] correlation $a=0.025$ m/s and $b=-1$, and in the Stemerding[14] correlation $a=0.003$ and $b=0$. In the case of dense suspensions it is likely that τ_p is determined by the collision of

clusters on the wall where inertial force is dominating. Therefore, in the present analysis we assume $a=0.003$ and $b=0$. On the other hand, the wall-gas shear stress τ_f can be neglected since it is already well known that the axial pressure drop $-dP/dz$ is almost equal to the weight of suspension $(1-\varepsilon)\rho_p g$ in a circulating fluidized bed.

1.6 Area fraction of annulus $(1-\alpha^2)$ from minimum pressure drop criterion

Adopting the minimum pressure drop criterion as in the analysis by Nakamura and Capes,[10] the fraction of cross-sectional area of the annulus can be determined. Eliminating β_c, β_a and τ_α, we have the following expression for pressure gradient parameter $E\equiv -(1/\rho_p g)(dP/dz)$ from Eqs. (8)–(11).

$$E\equiv -(1/\rho_p g)(dP/dz)$$
$$=\alpha^2(1-\varepsilon_c)+(1-\alpha^2)(1-\varepsilon_a)+4\tau_p/D_t\rho_p g \quad (18)$$

To satisfy the minimum pressure drop criterion the partial differentiation of E by $1-\alpha^2$ is equated to zero and the following equation is obtained:

$$1-\alpha^2=\frac{1}{\varepsilon_c^*-\varepsilon_a^*}\left[2(2+b)\lambda_p(1-\varepsilon_c^*)^{2+b}(1-\varepsilon_a^*)\right.$$
$$\times\left\{\frac{\varepsilon_c}{1-\varepsilon_c}v_0^+-u_0^++\varepsilon_c^{*n}\right\}$$
$$\left.\times\left|\frac{\varepsilon_c}{1-\varepsilon_c}v_0^+-u_0^++\varepsilon_c^{*n}-(\varepsilon_c^{*n}-\varepsilon_a^{*n})(1-\alpha^2)\right|^{1+b}\right]^{1/(3+b)} \quad (19)$$

where λ_p is defined as

$$\lambda_p\equiv\{2|\tau_p|/gD_t\rho_p(1-\varepsilon)\}/|v_a'/u_{tcl,c}|^{2+b}$$
$$=au_{tcl,c}^{2+b}/gD_t \quad (20)$$

2. Experimental

2.1 Equipment and methods

The laboratory-scale circulating fluidized bed used in the present work is shown in **Fig. 1**. The main column (riser), made of PMMA resin, was 50 mm I.D. and 2790 mm high. Circulation rate was measured by a semi-continuous particle flow meter which discharged particles from the weighing cone about every 10 seconds. The particle flow meter was designed so that it did not close the gas pressure loop while it was weighing particles. The particle circulation rate was controlled by aeration to the downcomer and a butterfly valve. The optical probes used for measuring cluster velocity and the particle concentration in the cluster phase are shown in **Fig. 2**. The optical fiber diameter was 0.5 mm. The effective distance between two light-detecting fibers determined by the method of Ohki *et al.*[11] was 3.1 mm. Cluster velocity was determined by the cross-correlation method, where the average delay time between the two signals from probe A was obtained by an FFT analyzer (A & D AD3521). The sampling frequency was 5 kHz. The total number of light reflection samples was 2048 for one correlation. To obtain an average delay time, 256 correlations were averaged.

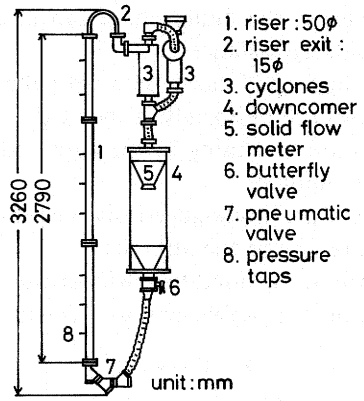


Fig. 1. Laboratory-scale CFB

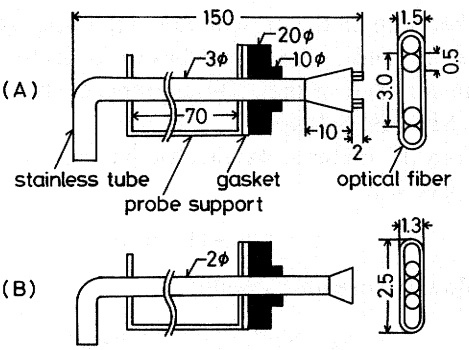


Fig. 2. Optical fiber probes
(A: for velocity; B: for concentration)

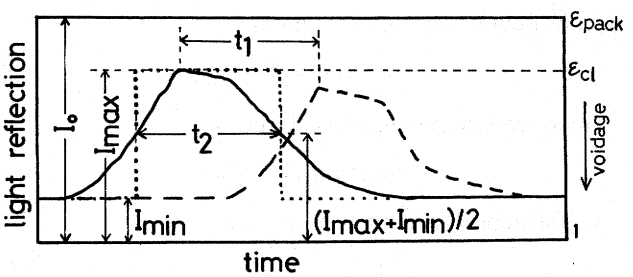


Fig. 3. Illustration of method to determine d_{cl} and ε_{cl} from light reflection signals

A cluster's size and its voidage, d_{cl} and ε_{cl}, were determined from light reflection outputs. The nominal "cluster diameter" d_{cl} was calculated by the following equation:

$$d_{cl}=1.5\times l\times t_2/t_1 \quad (21)$$

where parameters t_1 and t_2 were determined in the manner illustrated in **Fig. 3**. The factor 1.5 was used, assuming that the clusters were spherical.

For the conversion of light reflection intensity to void fraction, a calibration line discussed in the

following section was used. For the core 100 cluster samples at $r=0$ mm and for the annulus 33 samples at $r=24$ mm were taken to determine ε_{cl} and then ε^* from Eq. (7).

2.2 Calibration of the probe

As shown in **Fig. 4** the average delay time obtained by the FFT analyzer agreed fairly well with the average time lag between corresponding peaks of the original light reflection signals from the two probe tips.

Figure 5 shows the relationship between the cross-sectional area average of the time average intensity of light reflection and the average void fraction determined from pressure measurement.

The line in Fig. 5 was extrapolated to $\varepsilon=0.7$ and applied to convert the local instantaneous light reflection intensity into the particle fraction in the cluster phase. The peak intensity I_{max} shown in Fig. 3 was used to obtain ε_{cl} with the assumption of uniform voidage in a cluster.

3 Results

3.1 Radial velocity profiles

A typical pattern of the radial distribution of the delay time between light reflection signals from adjacent optical fibers is shown in **Fig. 6**(a). Observed examples are shown in Fig. 6(b). In the present work the radial point where the delay time becomes zero was taken as the core/annulus boundary. In the ideal situation the data should be those shown by the broken curves in Fig. 6(a).

Since around the core/annulus boundary the solid flow direction fluctuates quite often, the average value of the delay time τ from the cross-correlation method becomes zero at a certain radial point. To determine the velocity profile more precisely it is recommended to analyze the original light reflection signals directly with separate treatments for ascending and descending clusters.

The velocity profiles corresponding to Fig. 6(b) are shown in **Fig. 7**. It is obvious that a typical annular flow was established in the main column, which coincides with recent data of other investigators.[2,4,15]

3.2 Cluster size and voidage in the cluster

In **Table 1** the operating conditions and mean values observed at $z=1.06$ m are shown. The results on radial and axial distributions of solid holdup and average cluster size distribution can be found in the previous paper.[5] In **Fig. 8** the size and voidage of each cluster are shown for the case of $u_0=1.29$ m/s, $G_s=10.7$ kg/m^{2}s and probe height $z=1.06$ m. As can be seen in Fig. 8, the voidage in the cluster phase is independent of cluster size. Average cluster diameter and voidage are also listed in Table 1 with the nominal values of minimum fluidization velocity $u_{mf,cl}$ and terminal velocity $u_{t,cl}$ of clusters.

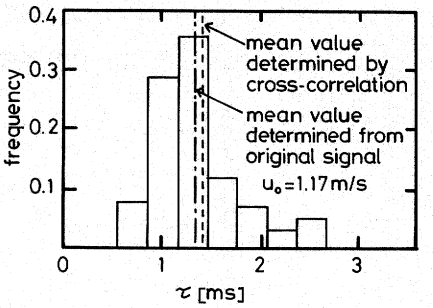


Fig. 4. Comparison of mean delay time determined from cross-correlation method and that from original light reflection signals

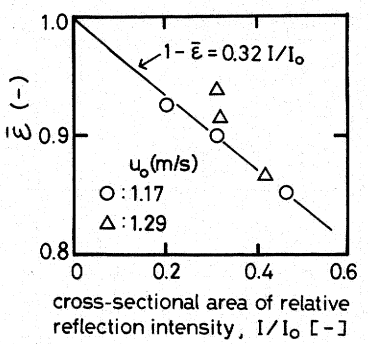


Fig. 5. Relation between cross-sectional area average values of ε and light reflection intensity

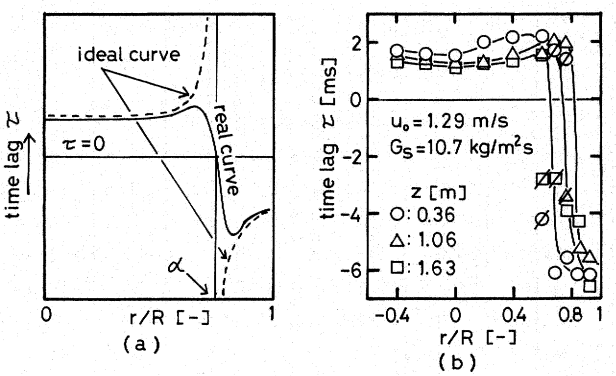


Fig. 6. Radial distribution of delay time corresponding to cluster velocity
((a): conceptual; (b): experimental)

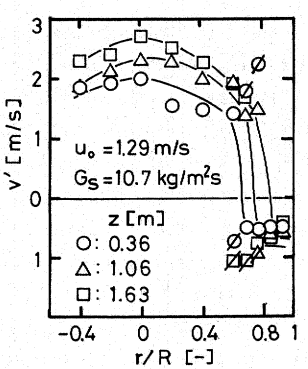


Fig. 7. Cluster velocity profiles
(Keys with slash denote temporary values.)

Table 1. Typical operating conditions and bed structure parameters

operating conditions	$u_0=1.29$ m/s $G_s=10.7$ kg/m^2 s	Particles: FCC $d_p=60\,\mu$m $\rho_p=1000$ kg/m^3
mean values	$d_{cl,c}=10.3$ mm	$\varepsilon_{cl,c}=0.85$
	($u_{tcl,c}=7.05$ m/s	$u_{mfcl,c}=0.82$ m/s)
observed	$d_{cl,a}=10.8$ mm	$\varepsilon_{cl,a}=0.76$
	($u_{tcl,a}=8.03$ m/s	$u_{mfcl,a}=0.94$ m/s)
at $z=1.06$ m	$\varepsilon_c=0.97$	$\varepsilon_c^*=0.81$
	$\varepsilon_a=0.82$	$\varepsilon_a^*=0.27$
	$\alpha=0.82$	$\lvert\partial v'/\partial r\rvert=340\,s^{-1}$

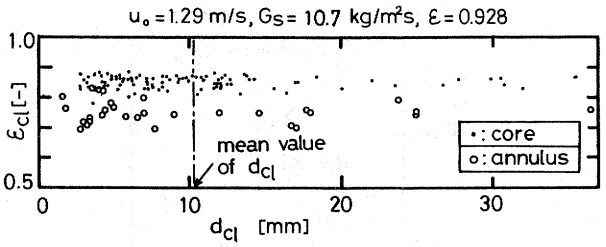


Fig. 8. Observed value of d_{cl} and ε_{cl}

Since the observed cluster size is sufficiently large, the following equations are adopted to estimate $u_{mf,cl}$ and $u_{t,cl}$:

$$u_{mf,cl}=\{d_{cl}(\rho_{cl}-\rho_d)g/24.5\rho_d\}^{1/2} \tag{22}$$

$$u_{t,cl}=\{3g(\rho_{cl}-\rho_d)d_{cl}/\rho_d\}^{1/2} \tag{23}$$

where $\rho_{cl}=\rho_p(1-\varepsilon_{cl})$ is the density of a cluster and ρ_d is the density of dilute phase. To obtain the values in Table 1 $\rho_d \doteqdot \rho_f$ was assumed. By using gas viscosity the apparent value of the Archimedes number for an average cluster listed in Table 1 is obtained as 7.5×10^6. This value is sufficiently large to adopt Eq. (23) for $u_{t,cl}$ and almost at the lower limit to adopt Eq. (22) for $u_{mf,cl}$.

4 Model Validation

4.1 Validation of Eq. (19) for $1-\alpha^2$ prediction

With experimental data α was calculated from Eq. (19). Results are shown in **Fig. 9** as a function of observed d_{cl}. When the parameter a is varied from 0.0012 to 0.006, the original value $a=0.003$ gives a fair prediction. As can be seen in Fig. 9 the agreement between the predicted value of α from average cluster diameter and the observed value of α is quite close. This indicates the validity of the CA model. Using the Konno-Saito[7] correlation for τ_p instead of that of Stemerding,[14] we obtain **Fig. 10**. It can be also seen from these figures that the value of α is rather insensitive to cluster diameter although it gradually decreased with increasing cluster diameter.

Concerning the drag coefficient of a cluster, if the value is determined mainly by the shape of the

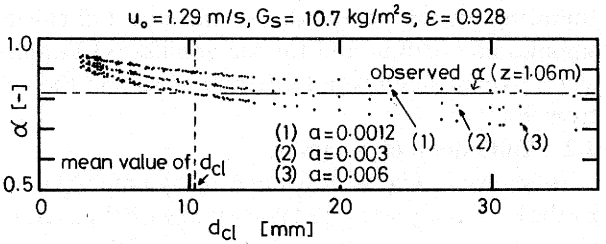


Fig. 9. Comparison of α observed and predicted from cluster data using Eq. (19)
(τ_p: Stemerding correlation)

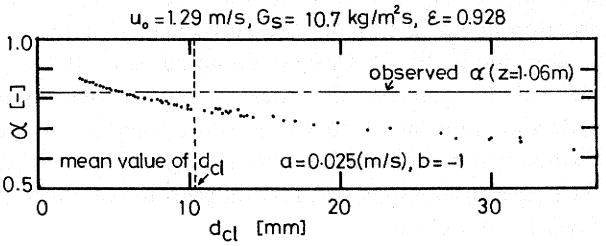


Fig. 10. Comparison of α observed and predicted from cluster data using Eq. (19)
(τ_p: Konno-Saito correlation)

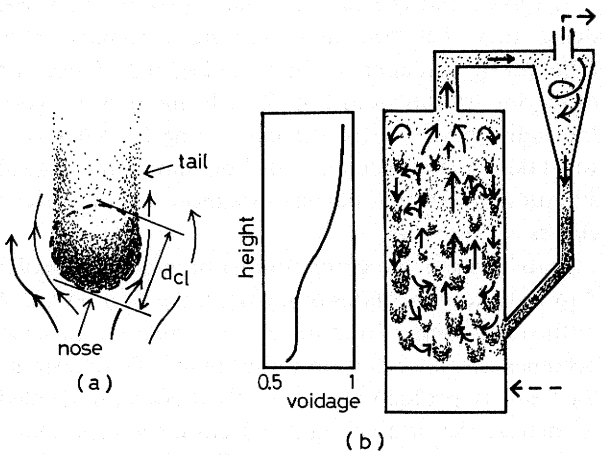


Fig. 11. Illustrations of present concepts of cluster and clustering annular flow ((a): spherical nose cluster; (b): fluidized clusters and voidage distribution)

spherical cluster nose and not by the cluster tail, the spherical cluster assumption in 1.1 would not contradict the realistic elongated shape of clusters which is illustrated in **Fig. 11**(a). From the values of $u_{t,cl}$ and $u_{mf,cl}$ shown in Table 1 it can be stated that most of the clusters in the main column are not transported but are only fluidized. The inflection point in the sigmoidal voidage distribution first reported by Li and Kwauk[8] may be referred to the bed surface of fluidized clusters. Above this level clusters of sufficiently small sizes or homogeneously suspended particles are transported to the column exit. Figure 11(b) illustrates this understanding of the cluster behavior in a CFB.

In Table 1 the value of $\varepsilon_a^*=0.27$ seems too low for packing of spheres. However, if the cluster tail is

elongated, such a low value would not be impossible.

4.2 Estimation of ε_d

In the above calculations gas density ρ_f was used for the dilute-phase density ρ_d. To examine the effect of the possible existence of particles in the dilute phase, calculations similar to those in the case of $a=0.003$ in Fig. 9 were performed for different ε_d. As can be seen from the result shown in **Fig. 12**, the observed α can be reproduced much better by the assumption $\rho_d=\rho_f$ (i.e. $\varepsilon_d=1$). It seems reasonable that when ε_d is decreased, the slip velocity between gas and cluster becomes smaller and the annular flow structure tends to disappear. Therefore, we can state that at least in the present model the assumption of no particles in the dilute phase holds.

The major problem left for future research is how to predict the cluster diameter and the voidage in the cluster.

4.3 Estimation of shear stress τ_α

In the present model τ_α was not neglected in the derivation of Eqs. (15) and (16). In this section τ_α is evaluated from the experimental data. Since the momentum of solid is quite large in comparison with that of gas, the stress between the annulus and the core can be approximately expressed by the Reynolds stress in the solid suspension. Applying Prandtl's theory and adopting the cluster diameter d_{cl} as the mixing length we have

$$|\tau_\alpha| = \rho_p(1-\varepsilon_c)d_{cl}^2 |\partial v'/\partial r|^2_{r=D_t\alpha/2} \tag{24}$$

and

$$\Gamma \equiv \frac{4\tau_\alpha}{(1-\varepsilon_c^*)\alpha D_t \rho_p (1-\varepsilon_{cl,c})g} = \frac{4d_{cl}^2}{\alpha D_t g}\left|\frac{\partial v'}{\partial r}\right|^2_{r=D_t\alpha/2} \tag{25}$$

If Γ is much less than unity, τ_α can be neglected in Eqs. (15) and (16). From experiments with a circulating fluidized bed of 50 mm I.D. and 2790 mm high, we have $|\partial v'/\partial r|_{r=D_t\alpha/2}=340\,\mathrm{s}^{-1}$. From the data of Werther *et al.*[3] for FCC particles in a CFB of 400 mm I.D. we have $|\partial v'/\partial r|_{r=D_t\alpha/2}=81\,\mathrm{s}^{-1}$. From the data of Knowlton *et al.*[6] for cracking catalyst in a circulating fluidized bed of 305 mm I.D. we have $|\partial v'/\partial r|_{r=D_t\alpha/2}=220\,\mathrm{s}^{-1}$. Here we take $|\partial v'/\partial r|_{r=D_t\alpha/2}=340\,\mathrm{s}^{-1}$ for rough calculation with FCC particle properties of $\rho_p=1000\,\mathrm{kg/m^3}$ and $d_p=60\,\mu\mathrm{m}$. The average cluster size in the core $d_{cl}=0.01$ m and $\alpha=0.82$ were known from experiment. Substituting these values into Eq. (25), we have $\Gamma=4{\cdot}0.01^2{\cdot}340^2/(0.82{\cdot}0.05{\cdot}9.8)=115$. Assuming $d_{cl}=0.01$–0.08 m and $\alpha=0.85$–0.90 from the experiments of Werther *et al.*[4] we have $\Gamma=0.74$–50. Since Γ is close to or much greater than unity, this rough estimation indicates that the shear stress at the core/annulus boundary τ_α cannot be neglected. Irrespective of the value of τ_α, the shear stress at the core/annulus boundary, the expression for $1-\alpha^2$ (Eq. (19)) remains unchanged. However, from Eqs. (8) and (15) the pressure gradient along the main column should be strongly affected by the core–annulus momentum exchange.

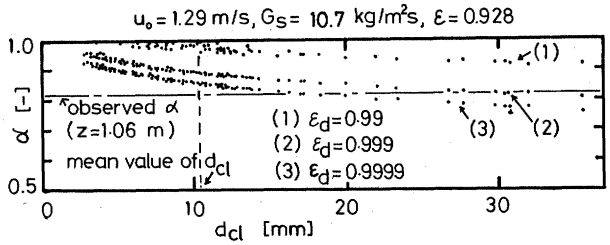


Fig. 12. Comparison of α observed and predicted from cluster data using Eq. (19) with varied ε_d (τ_p: Stemerding correlation)

Conclusions

The Clustering Annular Flow Model (CA model), in which a circulating fluidized bed is treated as a bed of homogeneously fluidized clusters, was derived and validated by experimental data. The following findings were obtained.

(1) The dimensionless core diameter α can be predicted by the CA model from the mean value of the nominal cluster diameter determined from measurements with the optical fiber probe.

(2) The friction factor f_p by the Stemerding correlation gave a fair prediction for the present core diameter data.

(3) The core/annulus shear stress τ_α cannot be neglected.

Nomenclature

a	=	defined by Eq. (17)	[—]
b	=	defined by Eq. (17)	[—]
d_p	=	mean particle size	[μm]
d_{cl}	=	cluster size	[m]
D_c	=	core diameter	[m]
D_t	=	column diameter	[m]
E	=	$-(1/\rho_p g)(dp/dz)$	[—]
f_p	=	$a\|v_a'\|^b$	[m/s]
g	=	acceleration of gravity	[m/s^2]
G_s	=	solid flow rate	[kg/m^{2}s]
l	=	probe distance	[m]
n	=	Richardson-Zaki parameter for cluster	[—]
P	=	pressure	[Pa]
r	=	radius	[m]
u'	=	u/ε	[m/s]
u, u_0	=	superficial gas velocity	[m/s]
u_{sl}	=	slip velocity	[m/s]
u_t	=	terminal velocity	[m/s]
u^+	=	$u_0/u_{tcl,c}$	[—]
v'	=	$v/(1-\varepsilon)$	[m/s]
v, v_0	=	superficial particle velocity	[m/s]
v^+	=	$v_0/u_{tcl,c}$	[—]
z	=	height	[m]

α	=	D_c/D_t	[—]
β	=	gas-cluster friction factor	[—]
ε	=	voidage	[—]
ρ	=	density	[kg/m^3]
λ_p	=	defined by Eq. (20)	[—]
τ_f	=	wall-gas shear stress	[Pa]
τ_p	=	wall-solid shear stress	[Pa]
τ_α	=	core-annulus shear stress	[Pa]
Γ	=	defined by Eq. (25)	[—]

〈Subscripts〉

a	=	annulus
c	=	core
cl	=	cluster
d	=	dilute phase
f	=	fluid
mf	=	minimum fluidization
p	=	particle
α	=	core/annulus boundary

〈Superscripts〉

*	=	cluster-free space
¯	=	cross section average

Literature Cited

1) Anderson, T. B. and R. Jackson: *Ind. Eng. Chem., Fundm.*, **6**, 527 (1967).
2) Bader, R., J. Findlay and T. M. Knowlton: Circulating Fludized Bed Technology II, ed. by P. Basu and J. F. Large, Pergamon, 123 (1988).
3) Grace, J. R. and J. Tout: *Trans. Inst. Chem. Eng.*, **57**, 49 (1979).
4) Hartge, E. U., D. Rensner and J. Werther: Circulating Fluidized Bed Technology II, ed. by P. Basu and J. F. Large, Pergamon, 165 (1988).
5) Horio, M., K. Morishita, O. Tachibana and N. Murata: Circulating Fluidized Bed Technology II, ed. by P. Basu and J. F. Large, Pergamon, 147 (1988).
6) Horio, M., Y. Kobukai, N. Yamanishi and A. Kasai: Preprints of 1st SCEJ Symp. on CFB, 20 (1987).
7) Konno, H. and S. Saito: *J. Chem. Eng. Japan*, **2**, 211 (1969).
8) Li, Y. and M. Kwauk: "Fluidization," J. R. Grance and J. M. Matsen (eds.), Plenum Press, 537 (1980).
9) Li, J.: "Multi-Scale Model and Method of Energy Minimization in Two-Phase Flow," doctoral dissertation, Inst. Chem. Met., Academia Sinica, Beijing (1987).
10) Nakamura, K. and C. E. Capes: *Can J. Chem. Eng.*, **51**, 39 (1973).
11) Ohki, K., K. Akehata and T. Shirai: Kagaku Kōgaku, **37**, 975 (1973).
12) Pritchett, J. W., T. R. Blake and S. K. Garg: *AIChE Symp. Ser.*, **74**, No. 176, 134 (1978).
13) Richardson, J. F. and W. N. Zaki: *Trans. Instn. Chem. Engrs.*, **35**, 35 (1954).
14) Stemerding, S.: *Chem. Eng. Sci.*, **17**, 599 (1962).
15) Weinstein, H., M. Shao and M. Schnitzlein: Circulating Fluidized Bed Technology, ed. by P. Basu, Pergamon, 201 (1985).
16) Yerushalmi, J., N. T. Cankurt, D. Geldart and B. Liss: AIChE Symp. Ser. **74**, No. 176, 1 (1978).
17) Yerushalmi, J., D. H. Tuner and A. M. Squires: *Ind. Eng. Chem. Process Dev.*, **15**, 47 (1976).